

DesignCon 2017

Design of Flyover QSFP (FQSFP) for 56+ Gbps applications

Kyoungchoul Koo, Missouri University of Science and Technology.
[kckoo84@gmail.com]

Pranay Vuppunutala, Missouri University of Science and Technology.
[pv6zf@mst.edu]

Atieh Talebzadehghahroudi, Missouri University of Science and Technology.
[ath27@mst.edu]

Jim Nadolny, Samtec, Inc.
[jim.nadolny@samtec.com]

Yuan Chen, Missouri University of Science and Technology.
[ycwnd@mst.edu]

Qian Wang, Xilinx Inc.
[qian.wang@xilinx.com]

James L. Drewniak, Missouri University of Science and Technology.
[drewniak@mst.edu]

Abstract

We introduce Flyover QSFP (FQSFP) approach for 56+ Gbps applications to overcome the limitations from a large loss on typical QSFP ports with surface mount to PCB traces. By replacing the PCB traces to the twinax cables, we have achieved 7 dB lower insertion loss at 40 GHz for the 12-inch path from the switch IC to connector than that of PCB trace with a low loss substrate. To investigate EMI aspect of FQSFP approach, we developed a simulation model of FQSFP. The model showed a good correlation with measured TDR at FQSFP port and TRP (total radiated power) from FQSFP in a test vehicle. TRP from FQSFP without a shielding cage is -8 dBW, -12 dBW at 15 GHz from 1 W input power for common-mode and differential-mode, respectively.

Author(s) Biography

Kyoungchoul Koo received the B.S., M.S. and Ph.D. degrees in electrical engineering, in 2006, 2008 and 2012, respectively, from Korea Advanced Institute of Science and Technology (KAIST), Daejeon, Korea. From 2012 to 2016, he worked at Samsung Electronics and developed design methodology for on/off-chip PI co-optimization in mobile SoC designs. He received the Best Paper Award at DesignCon 2014 and EDAPS 2015 and the Best Student Paper Award at EMC Compo 2011 and EMC 2011(2nd runner up). He is currently visiting research assistant professor at EMC group in Missouri S&T. His research interest includes Physics based system level power integrity optimization and estimation of EMI from a high-speed connector system.

Pranay Vuppunutala received his B.Tech degree in Electronics and Communication Engineering in 2015 from Jawaharlal University of Science and Technology (JNTU), Hyderabad, India. He is currently pursuing his M.S degree at EMC Laboratory, Missouri S&T. His primary research interests include the SI and EMI design of Flyover QSFP for 56 Gbps applications.

Atieh Talebzadeh received the B.S.E.E. degree from Shahed University, Tehran, Iran, in 2010, and the M.S.E.E. degree from Amikabir University of Technology, Tehran, in 2013. She is currently working toward the Ph.D. degree in electrical engineering at the EMC Laboratory, Missouri University of Science and Technology, Rolla, MO, USA. Her current research interests include ESD, EMC, signal Integrity, and antenna design. Ms. Talebzadeh was the recipient of 2015 technical paper award of ASHRAE. She won the first place award of IEEE EMC/SI student hardware design competition in 2016. She was a candidate for the best student paper award in the IEEE International Symposium on Electromagnetic Compatibility 2015.

Jim Nadolny received his BSEE from the University of Connecticut in 1984 and an MSEE from the University of New Mexico in 1992. He began his career focused on EMI design and analysis at the system and component levels for military and commercial platforms. His focus then shifted to signal integrity analysis of multi-gigabit data transmission. Jim is active within the technical community having served a 2 year term as chairman of TC-10, a technical committee dedicated to signal integrity in the IEEE EMC Society. Jim is a frequent presenter at DesignCon with Best Paper awards in 2004,

2008 and 2012 and has over 25 peer reviewed publications. At Samtec, Jim tracks technology trajectories via industry standards and other collaborations. Jim enjoys cooking, fishing, hunting and golf in the hills of Pennsylvania.

Chen Yuan received the B.S. degree in Electronic Commerce from Central China Normal University, Wuhan, Hubei, China in 2014 .She is currently working toward the Master degree in electrical engineering at EMC Laboratory, Missouri University of Science and Technology, Rolla, MO, USA. Her research interests include signal integrity in high-speed digital systems, Electromagnetic interference control.

Qian Wang received her B.S. and M.S. degree in Optics from Northwestern Polytechnical University, Xi'an, China, in 2009 and 2012, respectively. She joined EMC Laboratory at Missouri University of Science and Technology, Rolla, MO, USA in 2013 and received her M.S. degree in Electrical Engineering in July 2016. Her research interests include signal integrity study for silicon interposer technology and embedded multi-die interconnect bridge, high-speed signal design, EMI performance evaluation for high-speed devices.

James L. Drewniak received B.S., M.S., and Ph.D. degrees in electrical engineering from the University of Illinois at Urbana-Champaign. He is with Electromagnetic Compatibility Laboratory in the Electrical Engineering Department at Missouri University of Science and Technology (formerly University of Missouri-Rolla). His research and teaching interests include electromagnetic compatibility in high-speed digital and mixed-signal designs, signal and power integrity, electronic packaging, electromagnetic compatibility in power electronic based systems, electronics, and antenna design. He is a Fellow of IEEE.

Introduction

IEEE 802.3bs and IEEE 802.3cd are emerging Ethernet standards which aim to increase data transfer rates in networking equipment from 28 Gbps to 56Gbps [1]. This increase in data rate stresses traditional interconnects approaches and in this paper we consider the EMI aspects of an alternate interconnect approach. The traditional interconnect approach is known as Quad Small Form Factor Pluggable (QSFP). A lower loss interconnects solution has been developed which connects the front panel pluggable module to the switch ASIC using twinax cable. This category of cabled interconnect is referred to as “Flyover” as the high-speed signals “fly over” the lossy PCB traces. Figure 1 and Figure 2 illustrates the flyover QSFP (FQSFP) concept and the comparison between FQSFP and standard QSFP approaches.

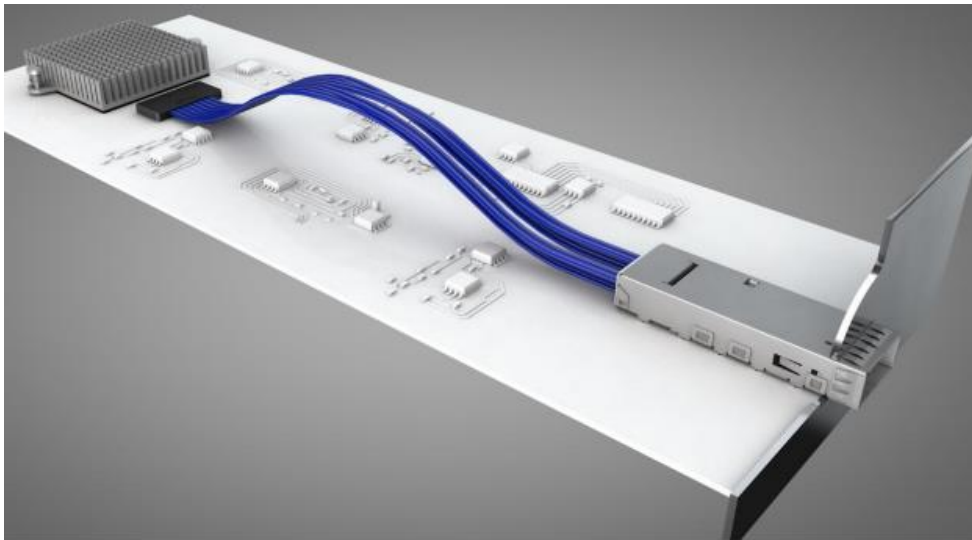


Figure 1. Implementation of Flyover QSFP on a PCB

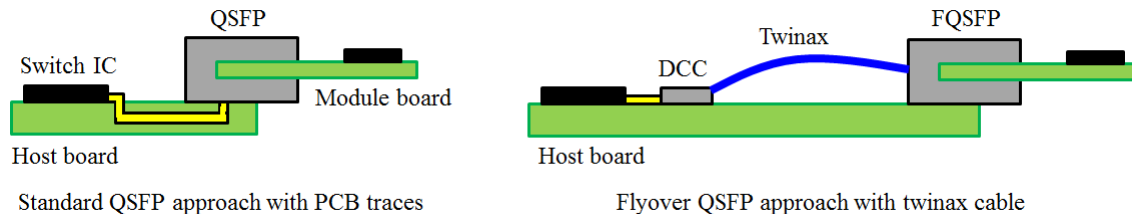


Figure 2. Comparison between standard QSFP and Flyover QSFP (FQSFP) approaches

The key to the lower loss FQSFP solution is the use of twinax cable which has a Teflon dielectric. Figure 3 shows a comparison of the insertion loss characteristics of twinax cable vs PCB traces on a Megtron6 PCB. At the 40 GHz, the insertion loss of 12-inch twinax cable in the FQSFP approach is 7 dB lower than typical 12 inch PCB trace in the low loss dielectric substrate in the standard QSFP approach. This lower loss FQSFP solution gives great advantages in the system design by enabling us to remotely locate the receiver. It gives much more system design flexibility. It enables us to have the higher

density port configuration (multiple stack), reduction of power consumptions by the elimination of re-timers, reduction of thermal dissipation by freeing designers to place ICs in preferred locations, reduction of PCB material costs due to lower layer counts and increased material options without losing the backwards-compatibility to standard QSFP.

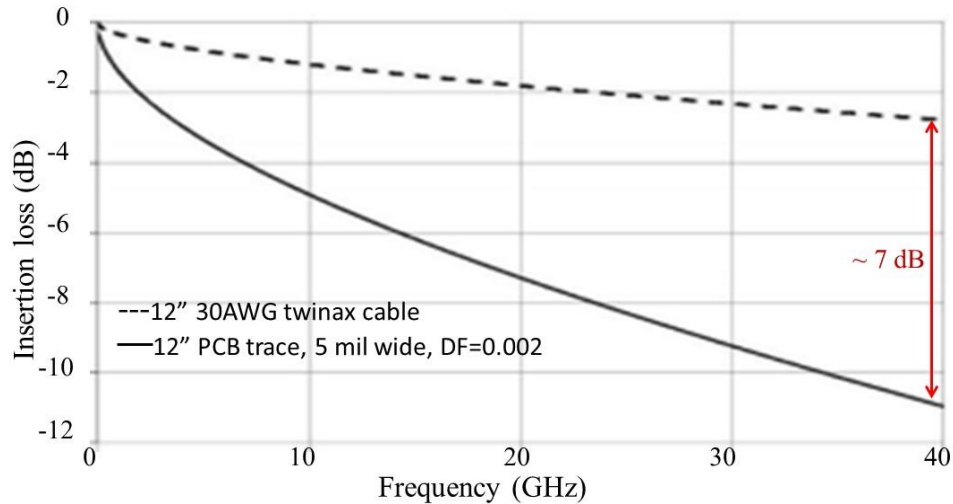


Figure 3. Insertion Loss Improvement of Twinax Cable compared to Copper Traces on a Megtron 6 PCB

The signal integrity aspects of this design are well predicted using modern full wave simulation tools. Product tradeoffs between SI performance, manufacturing approach and cost are routine in the product development process. What is novel and somewhat unique is the EMI aspect which is the subject of this paper. Typical applications in networking equipment may have 10's -100's of QSFP modules so we must engineer a solution assuming the combined emissions from many QSFP assemblies. Finally, we must assess the EMI impact of twinax cables penetrating the EMI cage which houses the QSFP module.

EMI characterization of QSFP

High-speed channel interconnect includes several impedance discontinuities at their connector and assemblies which act as an effective source of EM radiation [2]. Keeping the radiation below FCC regulation with those discontinuities is one of the most critical parts of high-speed channel system design. QSFP system also has several discontinuities at the interface between a module board and QSFP connector at host board, QSFP connector to twinax cable, and twinax cable to DCC connector right before IC. The EMI from those sources should be properly investigated and improved to meet the regulation before we complete the design cycle.

In this section, we introduce our test vehicle and a measurement correlated simulation model of QSFP for EMI characterization of QSFP. Once the model achieves the correlation with measurement, it enables us to perform simulation based design iterations, which is much more cost and time effective than trial and error on actual test vehicles, for further enhancement of EMI performance.

Design of test vehicle and simulation model: TDR

We designed a 4-layer PCB test vehicle with FQSFP approach. The test vehicle is fabricated and also modeled in CST microwave studio. Figure 4 shows the fabricated 4-layer PCB test vehicle with FQSFP connector and 6-inch long twinax cable. We have divided our work to get a measurement correlated simulation model into two parts, for TDR and for total radiated power (TRP). By doing the correlation work for TDR first, we could quickly screen out any errors in the signal path transition of the simulation model. These errors are generally difficult to troubleshoot directly from TRP simulation and measurement. Therefore, doing TDR first reduces our design iteration to achieve the measurement correlated simulation model for our EMI characterization of FQSFP.

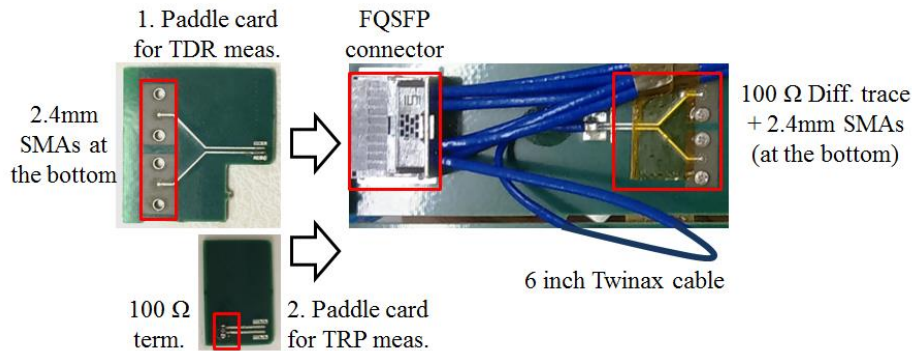


Figure 4. Fabricated 4-layer PCB test vehicle with FQSFP connector and 6-inch long twinax cable. Only one twinax (differential) cable is connected to the output SMA (2.4mm) ports on the right side. Two different types of paddle card (1, 2) are designed for TDR and TRP measurement, respectively.

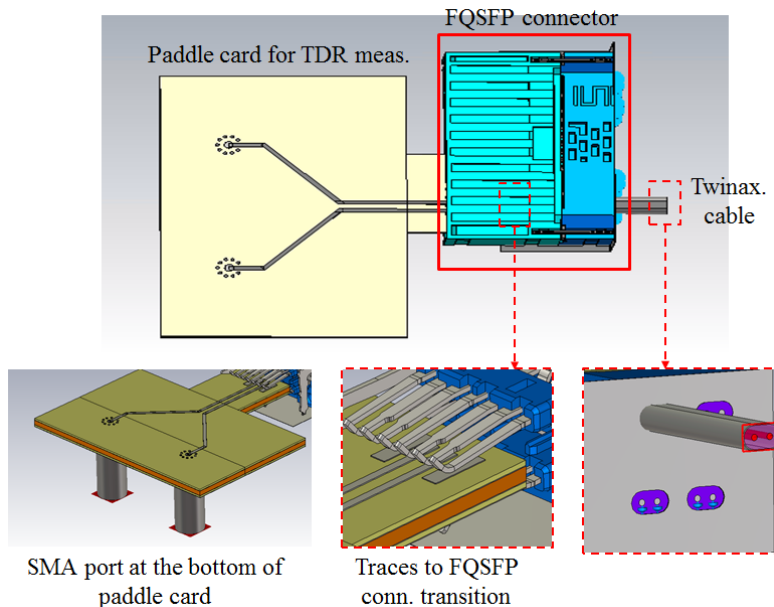


Figure 5. Simulation model of the test vehicle for TDR measurement in CST microwave studio. The model includes from SMA launch ports in the paddle card to the middle of twinax cable after FQSFP to reduce a simulation time. Therefore, TDR comparison with measurement only valid till the twinax cable. The material properties are given from PCB and FQSFP vendor.

Two different type of paddle card 1 and 2 were designed for TDR measurement and TRP measurement, respectively. These paddle cards play a role of the module board. The paddle card for TDR has SMA ports and the paddle card for TRP has 100- Ω termination resistor between differential trace pair. These paddle cards are plugged into FQSFP connector and terminate differential signal pins in FQSFP connector. This channel is connected to 2.4 mm SMA ports at the other end of the host board via 6-inch twinax cable. Figure 5 shows the corresponding simulation model with the paddle card for TDR measurement in CST microwave studio. The model only includes from SMA launch ports in the paddle card to the middle of twinax cable after FQSFP connector to reduce the simulation time. Therefore, simulated TDR comparison with measurement is only valid till the twinax cable. The material properties are given from PCB/FQSFP vendors. The simulation time of the model with CST took 3 to 5 hours depending on the resources of simulation machines. The simulation model and test vehicle for TRP will be explained in more detail later.

Simulation model updates from SEM cross-sectional analysis

The PCB traces in the test vehicle were originally designed to have 50 Ω single and 100 Ω differential characteristic impedance. However, the measured impedances at the single and differential traces in Figure 8 was 5~7 Ω lower than the design target value (100 Ω). After SEM cross-section analysis on the fabricated test vehicle, we found that the lower impedance was due to the thicker metal traces in the fabricated test vehicle than that of targeted in the design. Figure 6 summarizes the result of SEM cross-section analysis. The thickness of the trace was measured as 3.2 mil, which is more than two times larger than targeted value (1.4-mil), while space, width of traces vary within the range of 10% from the targeted value. The measured dimensions of traces are updated in the CST model before TDR simulation.

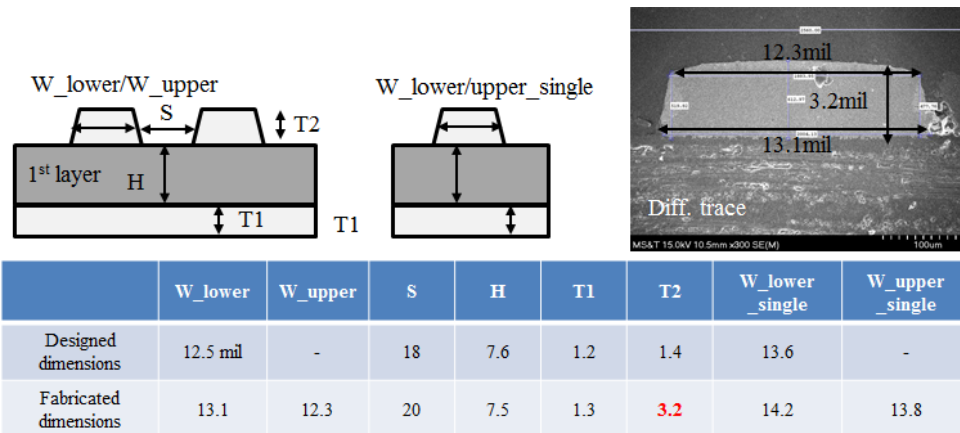


Figure 6. Cross-section of the fabricated test vehicle with SEM analysis. The thickness of traces was supposed to be 1.4 mil thickness for 100 Ω differential impedance but fabricated with 3.2 mil thickness

Measurement correlation of TDR

TDR measurement setup

To measure TDR profile of the test vehicle, we used a 50 GHz 4 ports VNA as shown in Figure 7. First, we measured 0.01~50 GHz 4 port S-parameter between two SMA ports at

the paddle card and the other two SMA ports at the host board. Then, it was converted to Differential TDR profile seen at SMA ports of the paddle card, using FEMAS tool, developed by EMC laboratory, Missouri S&T.

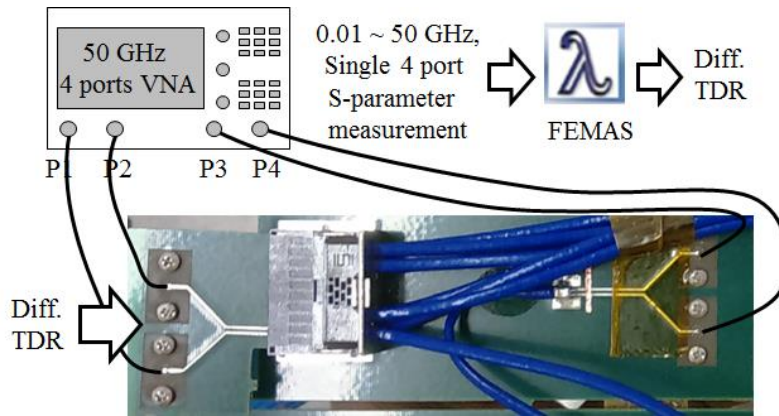


Figure 7. TDR measurement setup. We first measure 50GHz 4 port S-parameter of the differential channel from the SMA launches of paddle card to the other SMA launches at the host board after twinax cable. The measured S-parameter is converted to differential TDR seen at the SMA launches of paddle card by FEMAS tool developed by EMC lab, Missouri S&T.

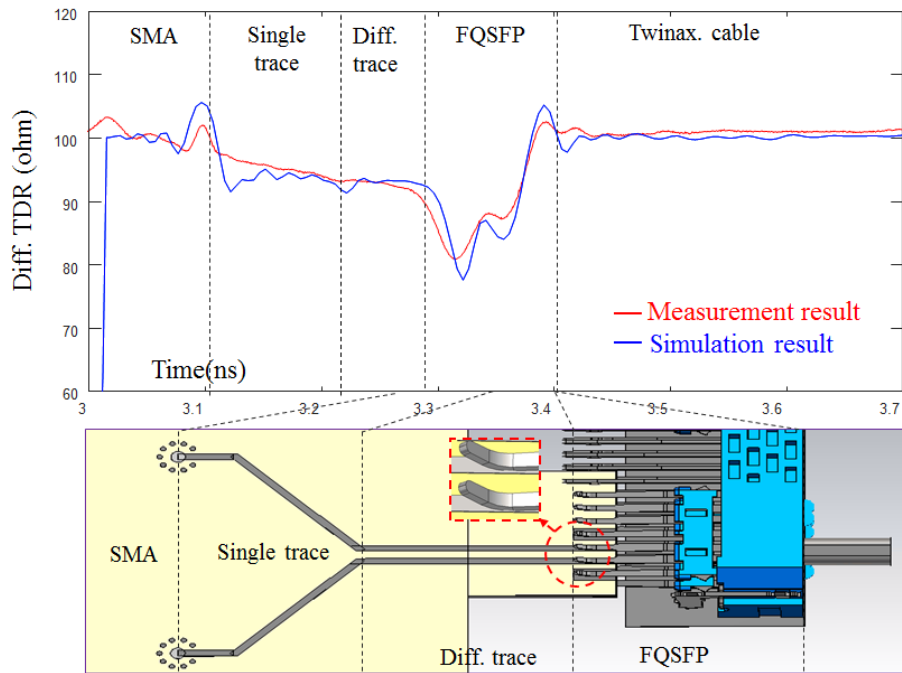


Figure 8. The simulated TDR curve in CST microwave studio (blue) shows a very good correlation with measurement TDR curve (red). The large capacitive dip at FQSFP connector part is caused from an excessive coupling capacitance between the pin structure of FQSFP and PCB traces at the transition.

Measurement vs Simulation

The comparison of TDR in Figure 8 shows good correlation between measurement and simulation. Since the simulation model only models from SMA launch ports in the paddle

card to the middle of twinax cable after FQSFP, TDR profile within this range is compared with the measurement. The differential impedance of the single/differential traces for TDR measurement is lower than 100Ω because of the fabrication variation in trace thickness as explained earlier. By updating the dimensions of traces from SEM analysis to CST model, we achieved the good correlation for this part of the TDR profile. A big capacitive dip at the interface of FQSFP connector and the paddle card is caused by an excessive capacitance due to coupling between the pin structure of FQSFP and PCB traces at the transition. Having a void at a ground plane under the differential traces at the transition point can help to reduce the capacitive dip.

Design of test vehicle and simulation model: TRP

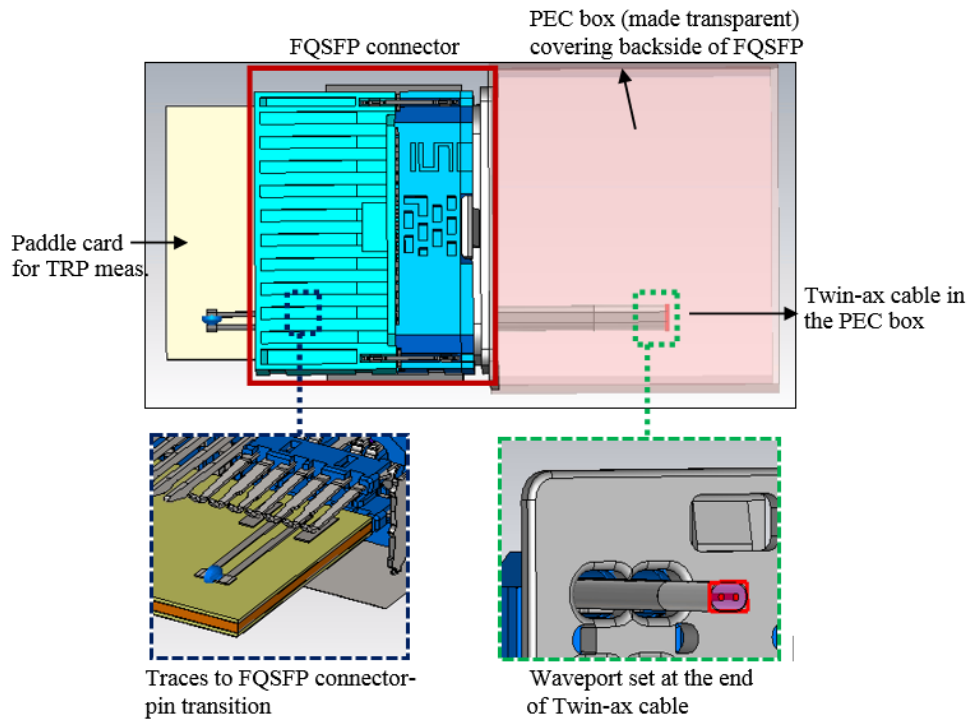


Figure 9. Simulation model of the test vehicle for TRP measurement in CST microwave studio. The paddle card plugged into FQSFP is terminated differentially with 100Ω lumped element. A waveguide port is set at the end of the twinax cable. The backside of FQSFP is covered with PEC box to isolate any EMI radiation from twinax cable and directly from the port.

Once we achieved the measurement correlation for TDR in the previous step, our next step is the correlation work for TRP from the FQSFP connector, which is an initial step to characterize the EMI of whole FQSFP system. To begin with, TRP was investigated from the FQSFP connector, targeting a favorable correlation ($\sim 3-5$ dB) between the measurements and simulations for both differential and common mode excitations. The simulations were carried out in CST microwave studio. The overview of the simulation model is shown in Figure 9. A paddle card plugged into FQSFP is terminated in 100Ω differential fashion for the differential mode as shown in Figure 4 and two- 50Ω single

ended fashion for the common mode. Such termination for common mode was to terminate the traces with defined common mode impedance.

Measurement correlation of TRP

TRP measurement setup

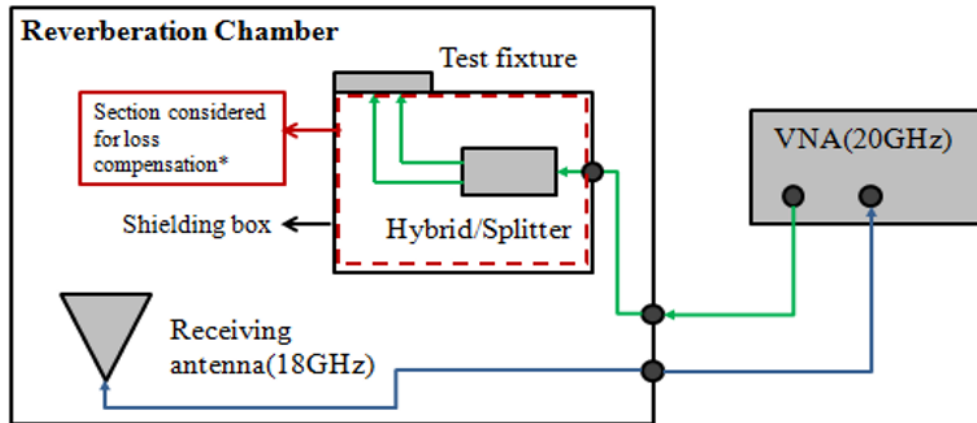
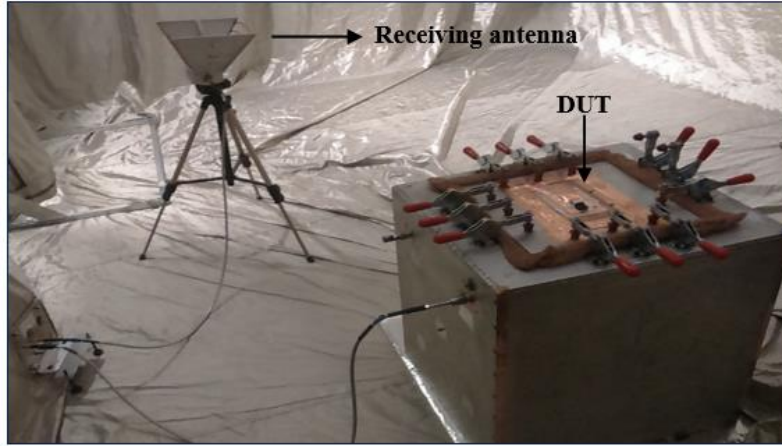


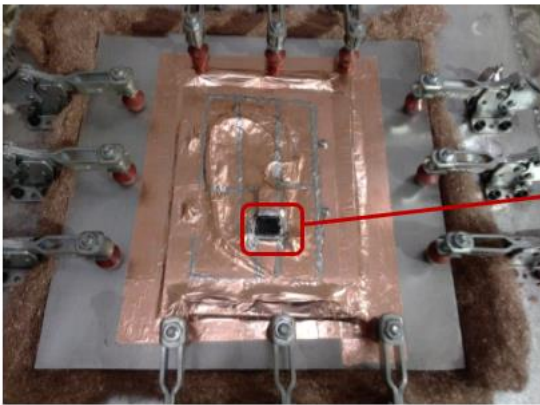
Figure 10. Block diagram of the measurement setup. A double-ridged horn antenna (750 MHz ~ 18 GHz) is used as a receiving antenna. The insertion losses of balun/splitter along with the SMA cables in the shielding box (highlighted red box in the figure) are compensated in the measurement result.

Besides the simulations, the TRP measurements were carried out up to 18 GHz in a stirred-mode reverberation chamber as setup schematic is depicted in Figure 10. The well-known TRP substitution method [3] was used to obtain TRP values. The receiving antenna limits the frequency band for TRP measurement to be 750 MHz to 18 GHz. A VNA (20 GHz) along with a balun (for differential mode) and splitter (for common mode) was used for the excitation of the test vehicle. In the simulation model, 0.5 W power is directly excited at end of the twinax cable. But in the measurement setup, there is an additional loss incurred due to the SMA cables and balun/splitter, in the highlighted red box in Figure 10. To account for these, the insertion loss of the cables and that of balun/splitter (~ 5.5 – 7.5 dB across the frequency range) is compensated on the measured TRP for the comparison with simulated TRP.

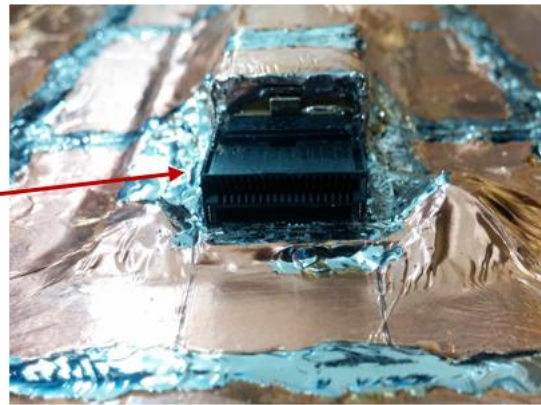
The actual measurement setup inside the stirred-mode reverberation chamber is shown in Figure 11 (a). In the test vehicle, except the FQSFP connector, everything else was shielded with copper tape as implied in Figure 11 (b). This was necessary to capture TRP only from the FQSFP connector. To ensure a reliable contact, the edges of each copper tape are soldered together as depicted in Figure 11(c).



(a)



(b)



(c)

Figure 11. (a) Measurement setup inside the reverberation chamber. The receiving antenna and FQSFP connector (DUT) is placed on the top of the shielding. (b) A close view of FQSFP connector in the measurement setup (c) FQSFP connector with backside shielded with copper tape and the edges of each copper tape are soldered together for better contact with each other.

Measurement vs Simulation

In order to provide the ease of comparison of the total radiated power (TRP) results, the input power to the FQSFP for both the simulated and measured TRP is re-normalized to 1W i.e., 0 dBW. After accounting for all the cables and balun/splitter losses on the measured TRP, the measurement and simulation results are compared in Figure 12. A favorable correlation of $\sim 3\text{-}5$ dB is observed in the case of common mode excitation. However, the differential mode has a significant difference of $\sim 5\text{-}10$ dB between measurement and simulation. After an investigation, it was found that the cause for such difference is the skew between two imperfect phase matched SMA cables from the balun to FQSFP connector, two green paths in the box in Figure 10. Considering the fact of high sensitivity of differential mode in a measurement setup due to phase imbalances along the signal lines, this skew can cause a differential to common mode conversion. Therefore, the measured TRP in differential mode setup is no longer pure differential mode and result in the larger TRP in the measurement than the simulated TRP with the pure differential mode excitation. The skew between the two SMA cables used after

balun is measured from the TDR (with 50 GHz BW) and found to be ~7 ps. In order to take account the skew into simulation setup, we set 7 ps skew between two ports in the simulation model, and the port setting was changed from waveguide port to discrete port.

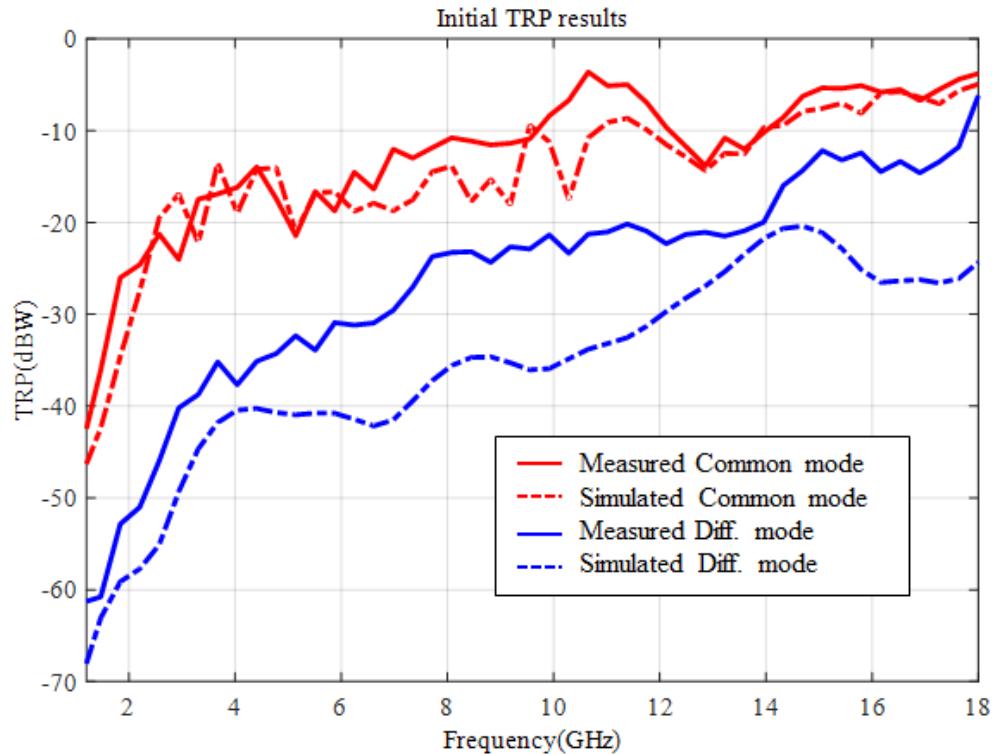


Figure 12. TRP comparison of measurement and simulation results. A favorable correlation of ~3-5 dB is observed for the common mode excitation. The ~5-10 dB difference for differential mode excitation is from the skew between two imperfect phase matched SMA cables from the balun to FQSFP connector. The skew can cause a differential to common mode conversion and result in the larger TRP in the measurement than the simulated TRP with the pure differential mode excitation.

After taking account the skew, the new simulated TRP shown in Figure 13 is higher than the previous case and hence much reasonable agreement was achieved with the measured TRP. The new correlation between measurement and simulation stands within ~3-5 dB for the differential mode. As long as the reflecting the skew into simulation model give us the good correlation with measured TRP, the simulated TRP without the skew in Figure 12 (blue solid curve) gives us an idea to predict a measured TRP with pure differential mode excitation. This amount of favorable correlation for both TDR and TRP profiles of the FQSFP proves that the model is ready to roll for the further simulation based enhancement of EMI design.

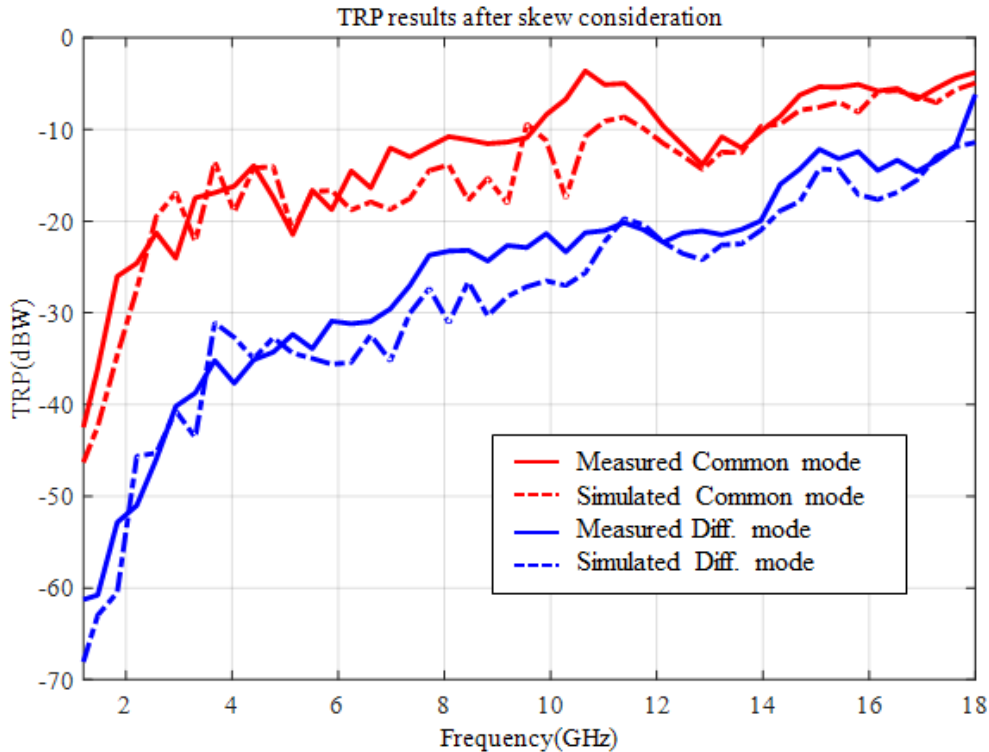


Figure 1. TRP comparison of measurement and simulation result with the skew compensation on the simulation. We set 7 ps skew, which is the measured skew between the two SMA cables used after balun is measured from TDR, between two ports in the simulation model. After taking account the skew, we achieved much reasonable agreement between the measurement and simulation, within ~3-5 dB for both the common and differential mode.

Summary

Flyover QSFP approach for 56+ Gbps application is introduced and compared with standard QSFP approach in terms of the insertion loss. Twinax cables in FQSFP offer about 7 dB lower insertion loss at 40 GHz for 12-inch path than the PCB traces in standard QSFP approach. Beside of the superior signal integrity performance of FQSFP, we have developed a simulation model of FQSFP to investigate another important aspect, EMI of FQSFP approach. We built a test vehicle to measure TDR and TRP of FQSFP and got a good correlation between the simulation and the measurements for both TDR and TRP from FQSFP. TRP from FQSFP without a shielding cage is -8 dBW, -12 dBW at 15 GHz from 1 W input power for common-mode and differential-mode, respectively. Once we have achieved the measurement correlated model for simulation, the simulation model facilitates a further simulation based enhancement of EMI design. The ultimate objective is to investigate the EMI for a real case implementation of FQSFP with high-speed data rates such as 28 Gbps, and extended up to 56 Gbps. For this purpose, proceeding to the next level in the EMI design of the FQSFP includes integration of cage, chassis, and optical module along with the current test vehicle and performing the same set of TRP experiments to corroborate simulations.

References

- [1] J. D'Ambrosia, "IEEE P802.3bs Baseline Summary", http://www.ieee802.org/3/bs/baseline_3bs_0715.pdf
- [2] Hall, Stephen H., and Garrett W. "Hall. High Speed Digital System Design: A Handbook of Interconnect Theory and Design Practices", Wiley, 2000.
- [3] G. Koepke, J. Ladbury, "Radiated Power Measurements in Reverberation Chambers", 56th ARFTG Conference Digest-Fall, vol. 38, pp. 1-7, 2000.